International Journal of Minerals, Metallurgy and Materials
Volume 26, Number 10, October 2019, Page 1266
https://doi.org/10.1007/s12613-019-1841-6

Influence of hot rolling on the microstructure of lean duplex stainless steel 2101

Zhi-jun Gao[1,2], *Jing-yuan Li*[1], *Zhi-hui Feng*[1], *and Yi-de Wang*[1,2]

1) School of material science and engineering, University of Science and Technology Beijing, Beijing, 100083, China
2) Institute of Engineering Technology, University of Science and Technology Beijing, Beijing, Beijing, 100083, China
(Received: 27 December 2018; revised: 26 March 2019; accepted: 2 April 2019)

Abstract: In this work, the microstructure and the strain partitioning of lean duplex stainless steel 2101 (LDX 2101) during different hot-rolling processes are investigated by optical microscopy and electron-backscattered diffraction (EBSD). The results show that the LDX 2101 exhibits poor thermoplasticity at high temperature. The four-pass hot-rolled plates show fewer edge-cracking defects and superior thermoplasticity compared with the two-pass hot-rolled plates prepared at different temperature. The phase boundary is the weakest site in the LDX 2101. The cracks are initiated and propagated along the phase boundaries during the hot-rolling process. According to the EBSD analysis, the increase of the hot-rolling pass can dramatically improve the strain distribution in ferrite and austenite phases and promote the strain transmission in the constituent phases, thereby improving the coordinated deformation ability of the two phases. This effect further increases the thermoplasticity and reduces the formation of edge cracks in LDX 2101.

Keywords: lean duplex stainless steel; hot-rolling process; thermoplasticity; strain distribution

1. Introduction

Duplex stainless steel (DSSs) is characterized by a ferrite (α) and austenite (γ) dual-phase structure at room temperature, which combines the advantages of austenitic stainless steels and ferritic stainless steels [1–5]. To achieve the best comprehensive properties, the α/γ phase ratio is generally approximately 1:1. DSS has high strength, high toughness, and excellent resistance to intergranular corrosion, pitting corrosion, and stress corrosion [6–8]. On the basis of its excellent properties, DSS is widely used in the petroleum, chemical, paper, subsea equipment, and other industries [9–10].

Lean duplex stainless steel (LDX) is a new type of DSS in which the element Ni is replaced by low-cost austenitizing elements N and Mn and the Mo content is reduced [11]. Although LDX 2101 is cost-efficient because it contains low concentration of Ni and Mo, its yield strength can reach twice that of traditional austenitic stainless steels such as AISI 304 while also ensuring good corrosion resistance [12–13]. However, compared with the traditional DSSs, the LDX 2101 exhibits worse thermoplasticity and more serious edge cracking during the rolling process.

Thermal processing, especially the hot-rolling process, is important for producing DSSs. Because of its dual-phase structure, the different crystal structures and stacking fault energy of ferrite and austenite phases lead to different deformation modes during the hot-rolling process. In general, the softening mechanism of the ferrite phase is dynamic recovery (DRV) because of its high stacking fault energy. Dislocations climb, and cross-slip easily occurs. By contrast, the austenite phase, which is characterized by low stacking fault energy, undergoes limited DRV. The major softening mechanism is dynamic recrystallization (DRX). Yang and Yan [14] have proposed that ferrite undergoes DRV and the grains become coarser during compression deformation at high temperature and that the austenite is softened by DRX. However, alternate interpretations of the softening mechanism in DSSs have been proposed. Liu *et al.* [15] have reported that continuous dynamic recrystallization (CDRX) is

Corresponding author: Jing-yuan Li E-mail: lijy@ustb.edu.cn

the major softening mechanism of both phases during hot compression. We observed that the small-angle boundaries gradually transformed into large-angle boundaries. Castan *et al.* [16] found that the softening mechanism of the ferrite phase has an important relationship with the Zener–Hollomon parameter (*Z*). Specifically, the ferrite undergoes discontinuous dynamic recrystallization (DDRX) at high *Z*-values, whereas CDRX occurs at low *Z*-values. Therefore, the hot-deformation mechanism of DSSs is complicated because of their two-phase structure.

In actual industrial production, DSSs usually require multipass rolling and the final deformation is achieved by multipass accumulation. In this paper, multipass hot-rolling tests of as-cast LDX 2101 were conducted at different temperature. The effects of the deformation temperature and the number of rolling passes on the microstructure, softening mechanism, and deformation coordination were investigated.

2. Experimental

The experimental material was LDX 2101 smelted in an argon oxygen decarburization furnace. The chemical composition is given in Table 1.

Table 1. Chemical composition of the LDX 2101 wt%

Steel	C	Cr	Ni	Mn	Mo	N	P	S	Si
LDX2101	0.033	22.0	1.28	4.52	0.13	0.222	0.009	0.0027	0.5
Standard	≤0.04	21–22	1.35–1.7	4.0–6.0	0.1–0.8	0.20–0.25	≤0.04	≤0.03	≤1.0

The multipass hot-rolling tests were carried out on a model 350 hot-rolling mill with hot-rolled slabs. The hot-rolled slabs were manufactured from the as-cast LDX 2101 with a length of 80 mm, a width of 40 mm, and a thickness of 20 mm. The slabs were soaked at 1100, 1200, and 1250°C for 30 min, followed by two-pass and four-pass hot-rolling processes. The final thickness of the plates was 5 mm. The reduction of each pass in the four-pass rolling process was 20%, 30%, 30%, and 30%, and the reduction of each pass in the two-pass rolling process was 40% and 60%. The finishing rolling temperature was 980°C. To retain the high-temperature microstructure, the plates were quenched immediately after the different hot-rolling processes. The hot-rolling process diagram is shown in Fig. 1.

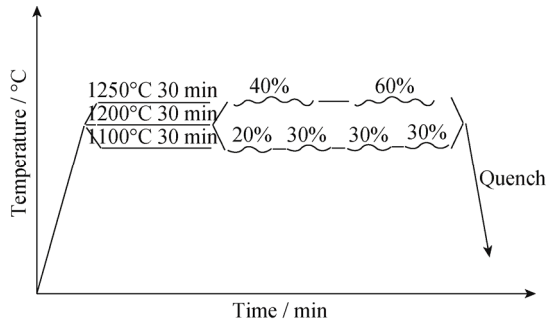

Fig. 1. Hot-rolling process for LDX 2101.

A Leica DM2500 optical microscope was used to observe the morphology. The specimens for optical observation were prepared by mechanical milling, polishing, and electrolytic etching in a 10wt% oxalic acid solution ($C_2H_2O_4$), which made the ferrite phase gray and the austenite phase bright. The etching potential was 7 V, and the current was 0.5 A. The deformation distribution and kernel average misorientation (KAM) distribution were analyzed with an LEO-1450 scanning electron microscope equipped with the Channel 5 electron-backscattered diffraction (EBSD) system. The specimens for EBSD analysis were prepared by mechanical polishing and electrolytic polishing with 10wt% perchloric acid and 90wt% glacial acetic acid solution. The potential was 20 V, and the current was 2.0 A. The volume fraction of ferrite phase was measured with a Feritscope FMP 30. Each specimen was measured ten times in different locations, and the average value was calculated. The phase diagram for LDX2101 was calculated using the Thermo-Calc software.

3. Results

3.1. The microstructure of as-cast LDX 2101

Fig. 2 shows the optical microstructure of as-cast LDX 2101. The island-shaped austenite is uniformly distributed on the ferrite matrix. In addition, the austenite phase also exhibits a dendritic morphology because of the as-cast condition. Because of the high content of alloying elements and the different partition coefficients of elements in two phases, DSSs are prone to form intermetallic phase [17]. Because of the low content of C and Mo in LDX 2101, the precipitation of the FeCr(Mo) (σ) phase and $M_{23}C_6$ phase is greatly suppressed; these two precipitates are not observed in the experimental material. The volume fraction of ferrite phase is 48.7%, as measured with a Feritscope, which means the α/γ phase ratio is approximately 1:1 in the as-cast LDX 2101.

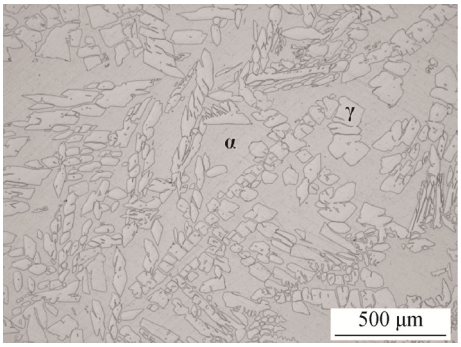

Fig. 2. Microstructure of the as-cast LDX 2101.

Fig. 3 shows the phase diagram of LDX 2101. During the hot-deformation process, whether the volume fraction of ferrite or austenite exceeds 20%, the thermoplasticity of the DSSs is drastically reduced, and defects such as cracks are prone to occur. When the α/γ phase ratio is approximately 1:1, DSSs exhibit its worst thermoplasticity [18]. Given the effect of the phase ratio and the precipitates on the thermoplasticity of the experimental material, we decided to carry out the multipass hot-rolling tests at different temperature of 1100, 1200, and 1250°C. The ratios of the ferrite phase in the experimental plates are 52.16%, 68.39%, and 77.31% at 1100, 1200, and 1250°C, respectively, as shown in Fig. 3.

3.2. The influence of hot-rolling passes on the microstructure

Fig. 4 shows the macroscopic morphology of the plate edge of LDX 2101 after two-pass and four-pass hot-rolling processes at different temperature. Compared with the four-pass hot-rolling process, two-pass hot-rolling process results in more edge cracks at the three investigated temperature. The edge macroscopic morphology of the experimental plate (Fig. 4(a)) shows that the thermoplasticity is obviously different after two-pass and four-pass hot-rolling processes, which is related to the evolution of the microstructures during different rolling processes. Fig. 4(b) shows the edge metallographic microstructure of the experimental plate at 1200°C after the two-pass hot-rolling process. All of the cracks are initiated at the phase boundaries and are extended along the phase boundaries. Clearly, the phase boundary is the weakest part of the LDX 2101. However, after two-pass hot rolling at 1100°C and 1200°C, a large number of cracks appear in the edge of the experimental plates, demonstrating poor thermoplasticity. When the temperature increases to 1250°C, the edge cracks of the experimental plate are greatly decreased and the thermoplasticity of the plate is improved.

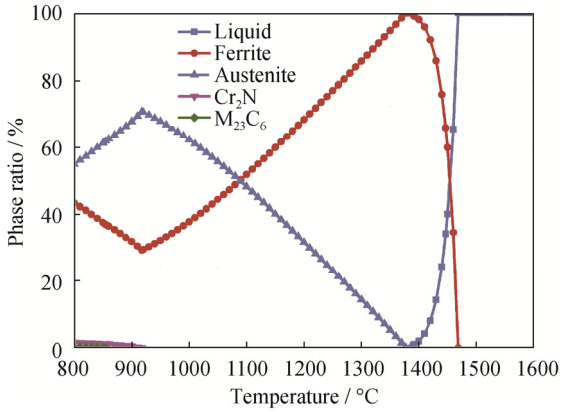

Fig. 3. Phase diagram of LDX 2101.

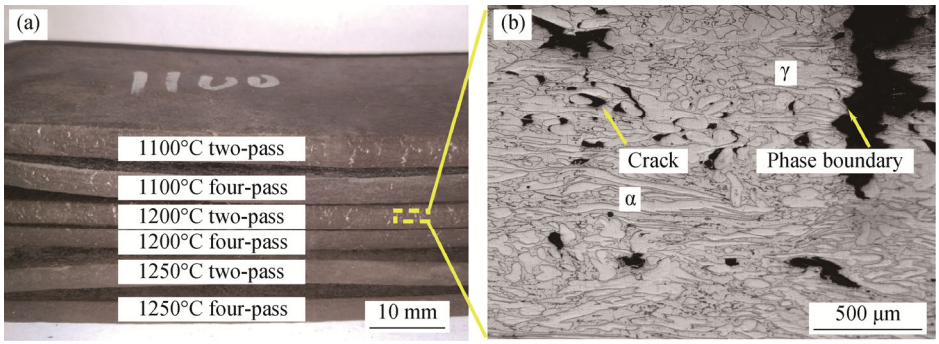

Fig. 4. The edge cracks after two-pass and four-pass hot-rolling processes at different temperature: (a) macroscopic morphology; (b) microcracks after two-pass rolling at 1200°C.

Chen *et al.* [19] have indicated that the ferrite phase ratio and thermoplasticity of DSSs increased with increasing temperature. Therefore, the edge cracks of the two-pass hot-rolled plate almost disappear at 1250°C. At the same temperature, the thermoplasticity of the four-pass rolled plate is better than that of the two-pass rolled plate, and the four-pass rolled plate exhibits fewer edge cracks. Thus, increasing the deformation temperature and the number of rolling passes can improve the thermoplasticity of the LDX 2101.

Fig. 5 shows the microstructures after two-pass and four-pass hot rolling of LDX 2101 at different temperature.

After the two-pass hot-rolling process at 1100°C (Figs. 5(a)–5(c)), the deformation of the austenite phase is small and the austenite phase is hardly deformed in the rolling direction. Block austenite remains distributed irregularly in the ferrite matrix, as shown in Fig. 5(a). The austenite and ferrite phases exhibit inhomogeneous deformation. However, after the four-pass hot-rolling process (Figs. 5(d)–5(f)), the austenite phase is obviously elongated along the rolling direction. The phase boundaries are distorted, and a large number of deformed banded structures appear.

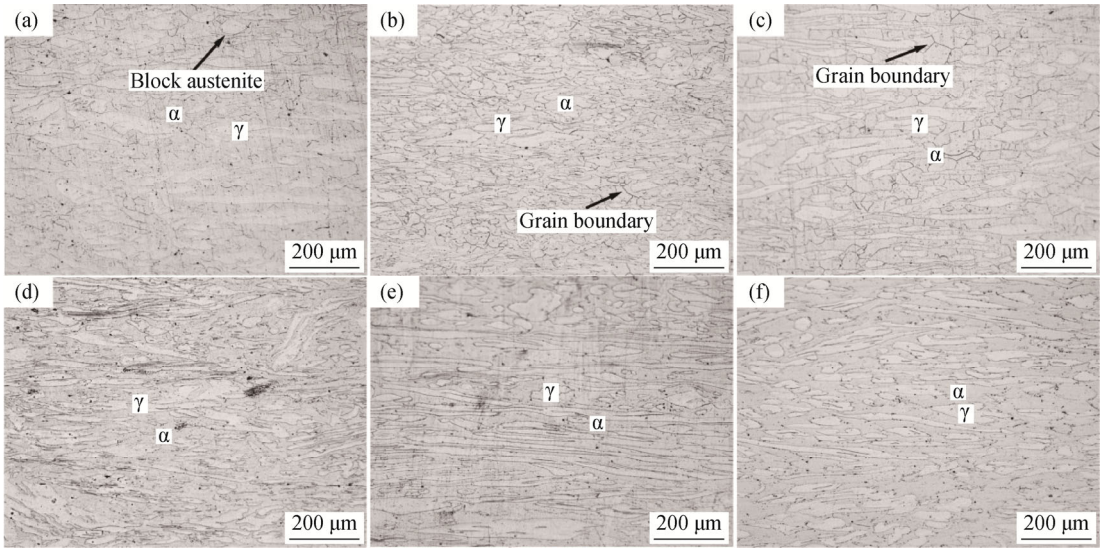

Fig. 5. Microstructures of LDX 2101 after (a–c) two-pass and (d–f) four-pass hot rolling at different temperature: (a,d) 1100°C; (b,e) 1200°C; (c,f) 1250°C.

When the hot-rolling temperature increases to 1200°C, the elongation of the austenite phase inside the ferrite matrix remains small after the two-pass hot-rolling process (Fig. 5(b)). The deformation characteristics are still not obvious. In addition, a few grain boundaries in the ferrite phase begin to appear, indicating that DRX has begun. After the four-pass hot-rolling process (Fig. 5(e)), compared with the hot rolling at 1100°C, the austenite phase is further elongated along the rolling direction and the plastic deformation increases. The austenite and ferrite phases exhibit homogeneous deformation, and the deformed banded structures are uniformly distributed.

At 1250°C, after the two-pass hot-rolling process (Fig. 5(c)), the amount of deformation of the austenite phase inside the ferrite matrix greatly increases and the austenite phase is elongated. The number of grain boundaries in the ferrite phase increases with increasing hot-rolling temperature and the degree of recrystallization increases. However, after the four-pass hot-rolling process (Fig. 5(f)), the austenite is broken along the rolling direction and the deformed banded structures are reduced.

Fig. 6 shows the microstructure of the LDX 2101 after two-pass and four-pass hot rolling at different temperature, as characterized by EBSD. A comparison of the distribution of the ferrite and austenite grain boundaries after different hot-rolling processes reveals that the ferrite grains are uniformly distributed and exhibit equiaxed morphology after a two-pass hot-rolling process at different temperature (Figs. 6(a)–6(c)), whereas the grain boundary distribution of the austenite phase is not uniform. No grain boundary is observed in the center of the large block austenite, whereas a large number of grain boundaries are concentrated near the grain edge region (marked by the arrow in Fig. 6). Additionally, with increasing temperature, the grain size of the ferrite phase increases. However, after the four-pass hot-rolling process (Figs. 6(d)–(f)), the grain boundary distribution of the ferrite phase is not uniform and a large number of grain boundaries are concentrated near the sharp corners of the ferrite phase boundary. In addition, a large number of grain boundaries also exist in the austenite phase. As the deformation temperature increases, the number of large blocks austenite decreases and the number of recrystallized grains with smaller grain sizes increases.

Consequently, the strain partitioning obviously differs in the ferrite and austenite because of the different rolling processes. In the case of the two-pass hot-rolling process, the ferrite phase accommodates more strain, which is prone to recovery and recrystallization. The austenite phase accommodates less strain, and the large block austenite phase remains in the ferrite matrix. However, the ferrite and auste-

nite phases are both in the deformed states during the four-pass hot-rolling process. The strain partitioning between the two phases is more homogeneous than that of the two-pass hot-rolling process. The number of large block austenite grains greatly decreases, and both phases exhibit a uniform banded structure, as shown in Fig. 6(f).

3.3. Deformation coordination and softening mechanism

Fig. 7 shows the deformation distribution of LDX 2101 after the two-pass hot-rolling process and the four-pass hot-rolling process at different temperature. To obtain the low-strain structure, substructure, and deformed structure, the angle thresholds for the substructure and deformed structure are 0° and 15°, respectively. The difference between the ferrite and austenite phases of the two-pass and four-pass hot-rolling processes is obvious at different temperature. After the two-pass hot-rolling process, the strain distribution in the two phases is substantially different. The ferrite phase is almost a low-strain structure (marked by blue), whereas the austenite phase is a substructure

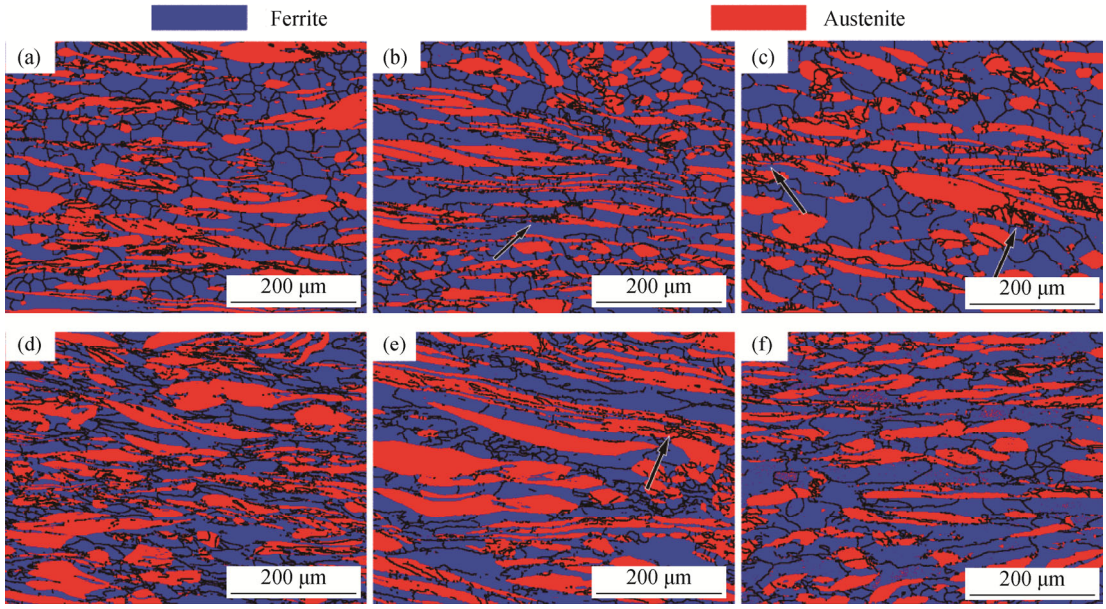

Fig. 6. The microstructure of LDX 2101 after (a–c) two-pass and (d–f) four-pass hot rolling at different temperature, as characterized by EBSD: (a,d) 1100°C; (b,e) 1200°C; (c,f) 1250°C. The black lines indicate grain boundaries.

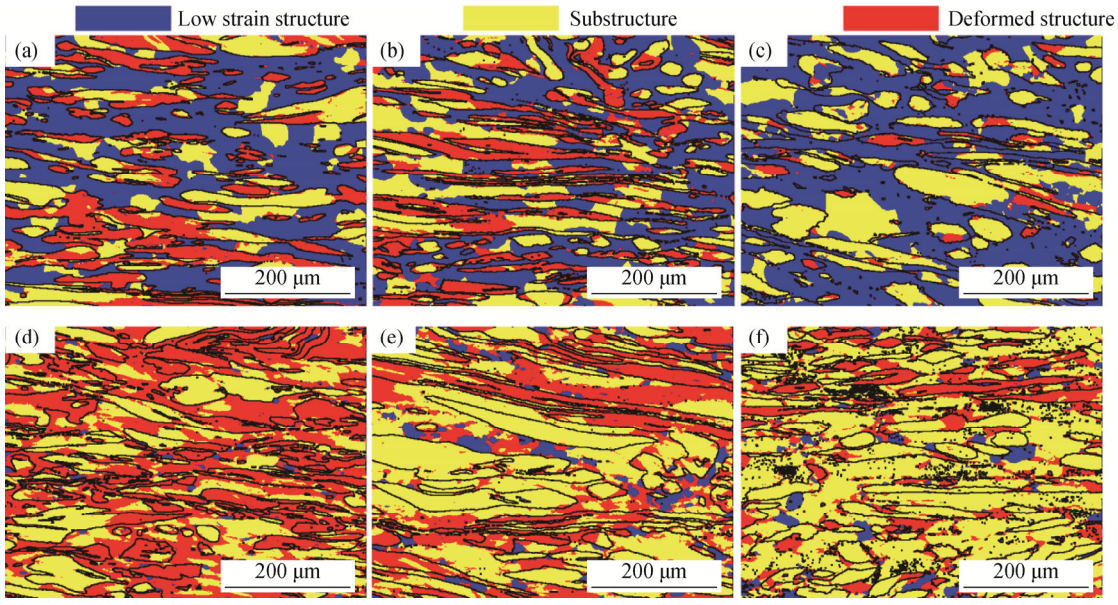

Fig. 7. The deformation distribution of LDX 2101 after (a–c) two-pass and (d–f) four-pass hot-rolling process at different temperature: (a,d) 1100°C; (b,e) 1200°C; (c,f) 1250°C. The black line indicates the phase boundary.

(marked by yellow) and a deformed structure (marked by red) with higher strain. After the four-pass hot-rolling process, the strain is uniformly distributed in the ferrite and austenite phases, both of which are substructures and deformed structures, with only a small amount of low-strain structure. Consequently, during the two-pass hot-rolling process, the deformation is largely concentrated in the ferrite phase and the deformation is difficult to transfer to the austenite phase, which leads to a large degree of recovery and recrystallization of the ferrite phase. However, the deformation of the austenite phase is not sufficient to trigger recrystallization; the austenite phase is still in the deformed state. On the contrary, the strain distribution of the ferrite and austenite phases is relatively uniform and both phases are in the deformed state during the four-pass hot-rolling process.

4. Discussion

The experimental results show that the effect of the hot-rolling passes on the thermoplasticity of LDX 2101 substantially changes the deformation distribution in the constituent phases. To further investigate the strain partitioning between the constituent phases, we analyzed the KAM after two-pass and four-pass hot-rolling process at 1250°C, as shown in Fig. 8. The distribution of KAM in the constituent phases is substantially different after different hot-rolling processes.

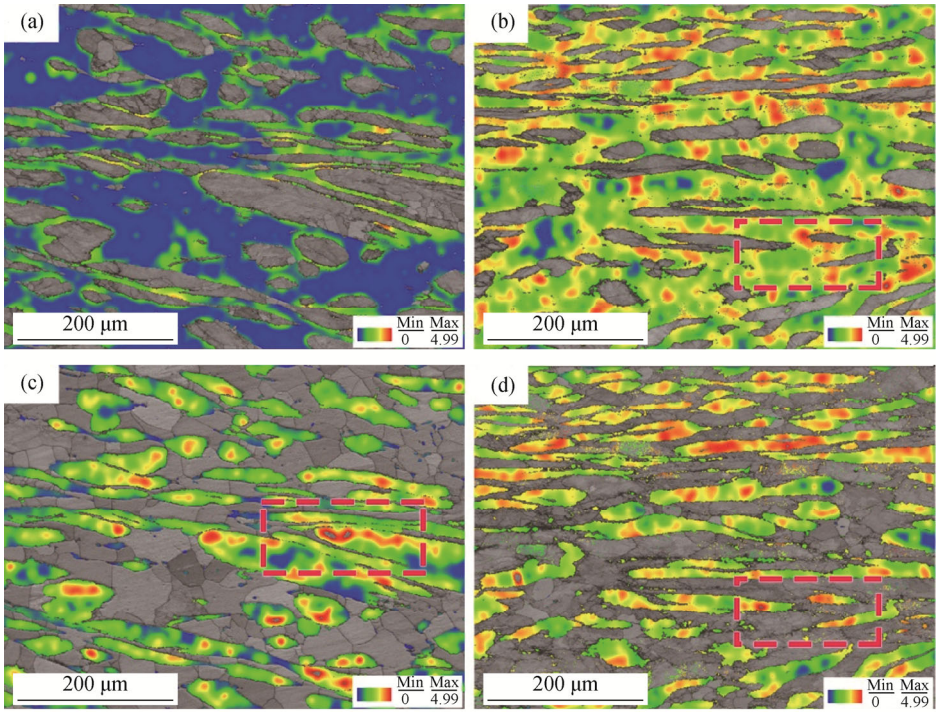

Fig. 8. The evolution of the KAM in the ferrite phase (a,b) and austenite phase (c,d) of LDX 2101 at 1250°C: (a,c) two-pass hot-rolling process; (b,d) four-pass hot-rolling process.

Compared with the four-pass hot-rolling process, the KAM in the ferrite phase is relatively low after the two-pass hot-rolling process and the high-KAM region is mostly concentrated in the austenite phase. The ferrite phase accommodates greater deformation during the two-pass hot-rolling process; thus, dynamic recovery and recrystallization occur. The dislocations generated by the deformation of ferrite with higher stacking fault energy are fully cross-slipped, the opposite sign dislocations are annihilated, and the same sign dislocations are rearranged so that the internal stress in the ferrite grain is released. The ferrite phase is kept in a low-strain state. The austenite accommodates less deformation and is difficult to recrystallize. The strain in the austenite is difficult to release, showing a high strain state. In addition, the austenite grain boundary is mostly the high-KAM region, whereas the ferrite grain boundary is the low-KAM region, resulting in stress concentration at the phase boundary.

By contrast, many researchers have found that the microhardness of the austenite phase is greater than that of the ferrite phase because of the difference in the nitrogen contents element and the different softening mechanisms [20–21]. During the two-pass hot-rolling process, the microhardness difference of austenite and ferrite increases further with increasing deformation. The strain is difficult to transfer from the ferrite phase to the austenite phase. The two phases are difficult to coordinate deformation, which reduces the thermoplasticity of LDX 2101, thereby causing the edge cracks during the hot-rolling process.

During the four-pass hot-rolling process, the KAM distribution of the constituent phases is homogeneous. Both phases have high-KAM value regions that are continuously distributed through the phase boundary, as marked by the box with the broken lines in Figs. 8(b) and 8(d). Ma *et al.* [22] found that the uniformity of the strain and microstructure distribution is an important factor affecting the hot-rolling property of DSSs plates. The increase of the hot-rolling pass effectively improves the strain distribution of the constituent phases. The strain is easier to transfer from the ferrite phase to the austenite phase during the four-pass hot-rolling process. The deformation of the constituent phases in LDX 2101 is coordinated, leading to better thermoplasticity. Therefore, the thermoplasticity of LDX 2101 is mainly affected by the strain distribution and softening mechanisms of ferrite and austenite during the hot-rolling process [23].

The thermoplasticity of DSSs is poor due to the dual-phase composition at high temperature, and different softening mechanisms of ferrite and austenite lead to inhomogeneous deformation. Iza-Mendia *et al*. [24] reported that ferrite is softer than austenite during hot deformation. The deformation is first concentrated in the ferrite phase, whereas the deformation of austenite phase is small, which leads to a compressive stress state of the ferrite grain and tensile stress state of the austenite grain. Stress is concentrated at the phase boundary so that cracks are easily generated. However, the body-centered cubic ferrite with high stacking fault energy tends to soften by dynamic recovery. The face-centered-cubic austenite tends to soften by DRX, which is only triggered when the strain accumulates to the critical strain. The different softening mechanisms of ferrite and austenite result in different work-hardening rates during the hot deformation. Feng *et al*. [25] reported that the recovery behavior of ferrite phase is much faster than austenite DRX. The difference in the softening degree further increases the stress concentration at the phase boundary, increasing the tendency of edge-cracking defects.

Fig. 9 shows the deformation mechanism during two-pass and four-pass hot-rolling processes. During the two-pass hot-rolling deformation, because of the large amount of deformation per pass, the accumulation of strain in the ferrite matrix causes a large degree of recovery and recrystallization, reducing the work hardening in the ferrite phase; by contrast, the strain inside the austenite phase is less and insufficient to trigger recrystallization; in this case, the work-hardening effect is greater. The heterogeneous distribution of the strain in the constituent phases causes the stress to be concentrated at the phase boundary. With increasing deformation, the strain in the ferrite phase is difficult to transfer to the austenite phase, eventually leading to edge cracks during the hot-rolling process. During the four-pass hot-rolling process, because of the small deformation per pass, the ferrite and austenite phases remain in the deformed state after each hot-rolling pass. The ferrite phase has a smaller degree of dynamic softening. Meanwhile, both phases undergo static recovery and recrystallization during the intervals of the hot-rolling process and the internal stress is reduced, which reduces the work-hardening effect. The constituent phases exhibit better deformation coordination and the strain is uniformly distributed in the two phases so that the experimental plate exhibits fewer edge cracks and better thermoplasticity during the four-pass hot-rolling process.

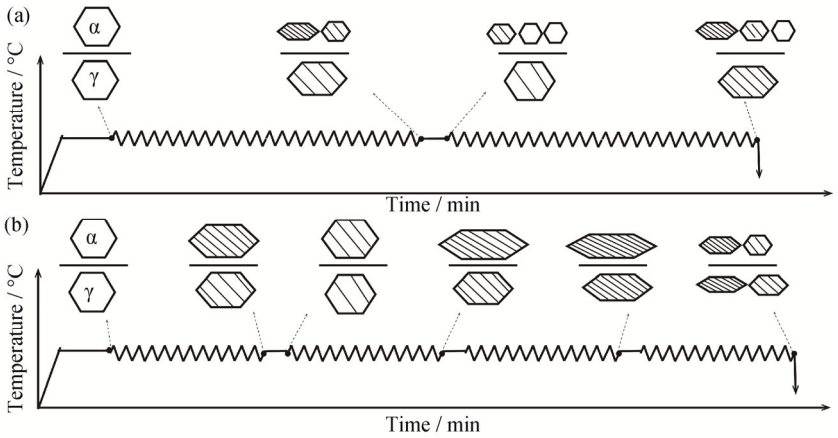

Fig. 9. Schematic of the microstructure evolution of LDX 2101 in (a) two-pass hot rolling and (b) four-pass hot rolling.

5. Conclusions

In this work, the microstructural evolution and the thermoplasticity of LDX 2101 during different hot-rolling processes are investigated in detail. On the basis of the experimental results, the main conclusions are as follows:

(1) Obvious edge-cracking defects are observed in LDX 2101 during hot-rolling process. Increasing the number of hot-rolling passes can substantially improve thermoplasticity of the experimental plate.

(2) Because of the different softening mechanisms and crystal structures of ferrite and austenite phases, the stress is concentrated in the phase boundary during the hot-rolling process. The α/γ interface is the weakest part of the LDX 2101, and the cracks are easily generated at the phase boundary.

(3) Compared with the two-pass hot-rolling process, the four-pass hot-rolling process exhibits better thermoplasticity because of the more uniform strain distribution and better deformation coordination of ferrite and austenite phases.

Acknowledgements

This research is financially supported by the National Natural Science Foundation of China (Nos. U1806220 and U1660114).

References

[1] S.S. Sohn, K. Choi, J.H. Kwak, N.J. Kim, and S. Lee, Novel ferrite–austenite duplex lightweight steel with 77% ductility by transformation induced plasticity and twinning induced plasticity mechanisms, *Acta Mater.*, 78(2014), p. 181.

[2] N. Jia, R.L. Peng, G.C. Chai, S. Johansson, and Y.D. Wang, Direct experimental mapping of microscale deformation heterogeneity in duplex stainless steel, *Mater. Sci. Eng. A*, 491(2008), No. 1-2, p. 425.

[3] Z.J. Gao, J.Y. Li, and Y.D. Wang, The crystallographic textures and anisotropy in 2507 super duplex stainless steel, *Steel Res. Int*,, 90(2019), No. 2, art. No. 1800397.

[4] Y. Zhao, W.N. Zhang, Z.Y. Liu, and G.D. Wang, Development of an easy-deformable Cr21 lean duplex stainless steel and the effect of heat treatment on its deformation mechanism, *Mater. Sci. Eng. A*, 702(2017), p. 279.

[5] S.F. Yang, Y. Wen, P. Yi, K. Xiao, and C.F. Dong, Effects of chitosan inhibitor on the electrochemical corrosion behavior of 2205 duplex stainless steel, *Int. J. Miner. Metall. Mater.*, 24(2017), No. 11, p. 1260.

[6] Y.S. Sato, T.W. Nelson, C.J. Sterling, R.J. Steel, and C.O. Pettersson, Microstructure and mechanical properties of friction stir welded SAF 2507 super duplex stainless steel, *Mater. Sci. Eng. A*, 397(2005), No. 1-2, p. 376.

[7] I.N. Bastos, S.S. Tavares, F. Dalard, and R.P. Nogueira, Effect of microstructure on corrosion behavior of superduplex stainless steel at critical environment conditions, *Scr. Mater.*, 57(2007), No. 10, p. 913.

[8] H. Miyamoto, T. Mimaki, and S. Hashimoto, Superplastic deformation of micro-specimens of duplex stainless steel, *Mater. Sci. Eng. A*, 319-321(2001), p. 779.

[9] K.H. Lo, C.H. Shek, and J.K.L. Lai, Recent developments in stainless steels, *Mater. Sci. Eng. R*, 65(2009), No. 4-6, p. 39.

[10] N. Zhou, R.L. Peng, and R. Pettersson, Surface integrity of 2304 duplex stainless steel after different grinding operations, *J. Mater. Process. Technol.*, 229(2016), p. 294.

[11] P. Cizek and B.P. Wynne, A mechanism of ferrite softening in a duplex stainless steel deformed in hot torsion, *Mater. Sci. Eng. A*, 230(1997), No. 1-2, p. 88.

[12] W. Zhang, L.Z. Jiang, J.C. Hu, and S. H.M. Song, Effect of ageing on precipitation and impact energy of 2101 economical duplex stainless steel, *Mater. Charact.*, 60(2009), No. 1, p. 50.

[13] H.J. Aval, Microstructural evolution and mechanical properties of friction stir-welded C71000 copper–nickel alloy and 304 austenitic stainless steel, *Int. J. Miner. Metall. Mater.*, 25(2018), No. 11, p. 1294.

[14] Y.H. Yang and B. Yan, The microstructure and flow behavior of 2205 duplex stainless steels during high temperature compression deformation, *Mater. Sci. Eng. A*, 579(2013), p. 194.

[15] Y.Y. Liu, H.T. Yan, X.H. Wang, and M. Yan, Effect of hot deformation mode on the microstructure evolution of lean duplex stainless steel 2101, *Mater. Sci. Eng. A*, 575(2013), p. 41.

[16] C. Castan, F. Montheillet, and A. Perlade, Dynamic recrystallization mechanisms of an Fe–8% Al low density steel under hot rolling conditions, *Scr. Mater.*, 68(2013), No. 60, p. 360.

[17] X.F. Wang, W.Q. Chen, and H.G. Zheng, Influence of isothermal aging on σ precipitation in super duplex stainless steel, *Int. J. Miner. Metall. Mater.*, 17(2010), No. 4, p. 435.

[18] Y.L. Chen, T.R. Zhang, Y.D. Wang, and J.Y. Li, Effects of O, N and Ni contents on hot plasticity of 0Cr25Ni7Mo4N duplex stainless steel, *Acta Metall. Sinica*, 50(2014), No. 8, p. 905.

[19] L. Chen, X.C. Ma, X. Liu, and L.M. Wang, Processing map for hot working characteristics of a wrought 2205 duplex stainless steel, *Mater. Des.*, 32(2011), No. 3, p. 1292.

[20] A. Momeni and K. Dehghani, Hot working behavior of 2205 austenite–ferrite duplex stainless steel characterized by constitutive equations and processing maps, *Mater. Sci. Eng. A*, 528(2011), No. 3, p. 1448.

[21] L. Duprez, B.C. De Cooman, and N. Akdut, Flow stress and ductility of duplex stainless steel during high-temperature torsion deformation, *Metall. Mater. Trans. A*, 33(2002), No. 7, p. 1931.

[22] M. Ma, H. Ding, Z.Y. Tang, J.W. Zhao, Z.H. Jiang, and G.W. Fan, Effects of temperature and strain rate on flow behavior and microstructural evolution of super duplex stainless steel under hot deformation, *J. Iron Steel Res. Int.*, 23(2016), No. 3, p. 244.

[23] J.A. Jiménez, F. Carreño, O.A. Ruano, and M. Carsí, High temperature mechanical behaviour of δ–γ stainless steel, *Mater. Sci. Technol.*, 15(1999), No. 2, p. 127.

[24] A. Iza-Mendia, A. Pinñol-Juez, J.J. Urcola, and I. Gutieérrez, Microstructural and mechanical behavior of a duplex stainless steel under hot working conditions, *Metall. Mater. Trans. A*, 29(1998), No. 12, p. 2975.

[25] Z.H. Feng, J.Y. Li, and Y.D. Wang, The microstructure evolution of lean duplex stainless steel 2101, *Steel Res. Int.*, 88(2017), No. 12, art. No. 1700177.